

HELICITY DEPENDENCE OF THE $N\pi(\pi)$ PROCESSES ON THE PROTON: NEW RESULTS FROM MAINZ

P. PEDRONI

for the GDH and A2 Collaborations

*INFN-Sezione di Pavia
via Bassi 6,
I-27100, Pavia, Italy
E-mail: pedroni@pv.infn.it*

A high quality double polarization data set for the helicity dependence of the total and differential cross sections for both $\gamma p \rightarrow N\pi$ channels in the Δ region has been obtained in the framework of the GDH experiment. The experiment, performed at the Mainz microtron MAMI, used a 4π detection system, a circularly polarized photon beam, and a longitudinally polarized frozen-spin target. The more recent results will be presented, with a particular emphasis on the second resonance region.

1. Introduction

The excitation spectrum of the nucleon has been the subject of many experimental and theoretical studies over the years. A precise knowledge of the properties of the nucleon resonances is a prerequisite for a complete understanding of the nucleon itself. Among the tools best suited to study these properties are pion production processes in both electromagnetic (γN , $\gamma^* N$) and hadronic (πN) reactions. A large data set, mainly for single pion production, combined with extensive partial-wave analyses and theoretical models has provided valuable information such as the Breit-Wigner masses, decay widths, and decay amplitudes for numerous resonances (e.g. P_{33} , S_{11} , D_{13} , ...). In several cases, however, the precision with which the resonance properties are known is still rather poor¹. This is especially true for the higher lying and strongly overlapping resonances that couple more weakly to the photon and show up in the double pion production region.

Since the resonance properties are helicity dependent, valuable new input to disentangle and study these resonances is provided by the helicity de-

pendence of single and double pion photoproduction using polarized beams and polarized targets.

In addition, the measurement of the helicity dependence of the $N\pi(\pi)$ channels will give a deeper insight into the dynamics contributing to the fundamental Gerasimov-Drell-Hearn (GDH) sum rule for the nucleon^{2,3}, which provides a crucial test for our understanding of the γ - N interaction.

The aim of the GDH collaboration^a is to provide an extensive data set of helicity dependent cross sections for all the partial and the total reaction channels both on the proton and on the neutron with a combined use of the MAMI (Mainz) ($m_\pi \leq E_\gamma \leq 800$ MeV) and ELSA (Bonn) ($600 \text{ MeV} \leq E_\gamma \leq 3$ GeV) accelerators.

In the following, results obtained for single and double pion production processes on the proton will be presented. Results on the experimental check of the GDH sum rule both on the proton and on the neutron can be respectively found in the presentations of K.Helbing⁴ and O.Jahn⁵.

2. Experimental setup

Only the main characteristics of the experimental setup are given here, while more details may be found in Refs. ^{6,7}. The experiment was carried out at the Glasgow-Mainz tagged photon facility of the MAMI accelerator in Mainz. Circularly polarized photons are produced by bremsstrahlung of longitudinally polarized electrons. A strained GaAs photocathode routinely delivered electrons with a degree of polarization of about 75%⁸. The electron polarization was monitored with a precision of 3% by means of a Moeller polarimeter. The photon polarization was evaluated according to Ref. ⁹. The photon energy was determined by the tagging spectrometer having an energy resolution of about 2 MeV¹⁰. The tagging efficiency was continuously monitored during the data taking by an e^+e^- pair detector installed downstream of the main hadron detector.

A butanol (C_4H_9OH), frozen-spin target¹¹ provided the polarized protons. The system consisted of a horizontal dilution refrigerator and a superconducting magnet ($\cong 2.5T$), used in the polarization phase, together with a microwave system for dynamic nuclear polarization. During the measurement the polarization was maintained in the frozen-spin mode at a temperature of about 50 mK and a magnetic field of 0.4 T, supplied by a

^aThis collaboration is formed by researchers from the Universities of Mainz, Bonn, Bochum, Erlangen, Göttingen, Lund, Nagoya, Tübingen and from INFN-Sezione di Pavia, RUG Gent, CEA Saclay, INR Moscow.

small superconducting holding coil inside the cryostat. The proton polarization was measured using NMR techniques with a precision of 1.6%. A maximum polarization close to 88% and relaxation times in the frozen-spin mode of about 200 h have been regularly achieved.

Photoemitted hadrons were registered in a large acceptance detector DAPHNE ¹² (see Fig. 1). DAPHNE is a charged particle tracking detector covering the full azimuthal angular region and polar angles θ_{lab} from 21° to 159° .

It consists of three cylindrical multiwire proportional chambers, surrounded by segmented plastic scintillator layers and by a scintillator-absorber sandwich. To increase the acceptance for the forward angular region, the additional forward detectors, the silicon microstrip detector MIDAS ¹³, an aerogel Cerenkov counter to suppress electromagnetic background, and the annular ring detector STAR ¹⁴ were installed, followed by a forward scintillator-lead sandwich counter.

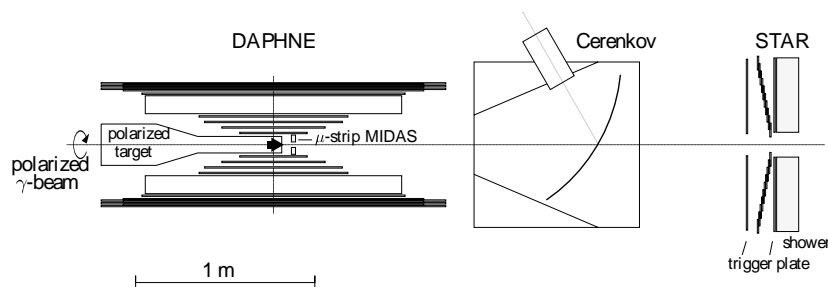


Figure 1. Schematic side view of the experimental setup of the GDH experiment in Mainz.

3. Data analysis

Charged particles stopped inside the central DAPHNE detector were identified using the range method ¹⁵, a maximum likelihood algorithm that uses simultaneously all the charged particle energy losses in the DAPHNE scintillator layers to discriminate between protons and π^\pm and determine their kinetic energies.

Since at least two energy loss samples along the charged track are needed, the domain of applicability of this method is restricted to particles that penetrate beyond the first scintillator layer. Protons stopped in the

first scintillator layer were then identified by using a standard $dE/dx - E$ technique, in which the wire chambers provide the dE/dx information and the first scintillator layer provides the E information¹⁶.

The identification of the charged particles that have sufficient energy to escape the detector was performed by using the $\Delta E - E$ technique described in¹⁷ which compares information provided by the geometrical path of the particle inside the detector with the energy deposited in the thickest scintillator layer.

The π^0 was identified by requiring a coincidence between the two photons resulting from its decay. For all π^0 energies and angles a fraction of these photons is detected inside our apparatus.

Non relativistic charged particles entered the MIDAS detector were identified by applying the range method developed for DAPHNE and adapted to MIDAS geometry¹³.

In the analysis of the data from the polarized butanol target, the background contribution from the reactions produced on the unpolarized C and O nuclei of the target could not be fully separated from the polarized H contribution¹⁸. However this background, coming from spinless nuclei, is not polarization dependent and cancels when the difference between events in the 3/2 and 1/2 helicity states is taken.

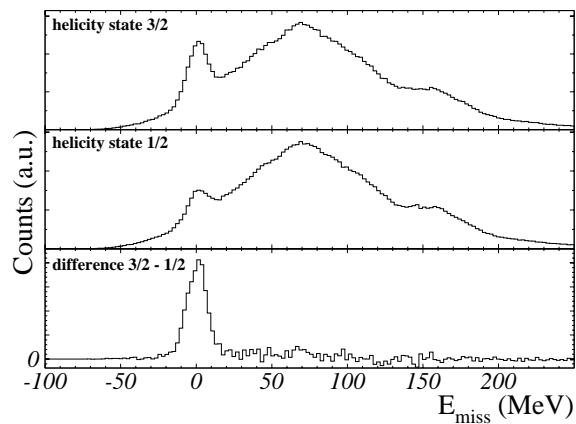


Figure 2. Missing energy spectra for the reaction $\bar{\gamma}p \rightarrow p\pi^0$ under the assumption that the proton originated from a reaction on a free proton. The spectra are shown for both helicity states and their difference.

As an example, Fig.2 shows this difference in E_{miss} (missing energy) obtained from events with a photoemission proton emitted in the Δ region and detected inside DAPHNE. E_{miss} is the difference between the measured proton kinetic energy and the proton kinetic energy evaluated (using E_γ and the polar emission angle) under the assumption that the proton originated from a π^0 production process on hydrogen. Missing energy distributions are shown for both helicity states and for their difference. The region outside the peak at $E_{miss} = 0$ corresponds to quasi-free reactions on C and O nuclei and has a yield consistent with zero in the difference spectrum.

4. Results and discussion

4.1. *Single pion photoproduction in the Δ region*

The photon energy region from pion production threshold to about 450 MeV, has been studied extensively over many decades. Several precise measurements, including those of single polarization observables, have been carried out, the main multipoles should be well determined. Therefore, we cannot expect to find big surprise when looking at the helicity dependent observables. These data then represent a consistency check of our new double polarization data and serve as a basis to improve our knowledge of the less important multipoles, like E_{1+} , for which our data has a good sensitivity.

An example of such a sensitivity is shown in Fig. 3 where our experimental results ⁷ are compared to three different predictions of the HDT theoretical analysis ¹⁹ in which the ratio between the (dominant) magnetic dipole (M1) and the (small) electric quadrupole radiation (E2) components of the proton $\rightarrow \Delta$ transition has been varied. The data are well reproduced with an E2/M1 ratio of -2.5%.

4.2. *Single pion photoproduction in the $D_{13}(1520)$ region*

At photon energies in the second resonance region (E_γ between 500 and 900 MeV), new information can be gained since, in this case, the resonance properties are known with much less precision. The helicity difference reveals a high sensitivity to the $D_{13}(1520)$ resonance. The multipoles E_{2-} and M_{2-} (E1 and M2 transitions respectively) are related to the helicity amplitudes in the following way:

$$A_{1/2}(D_{13}) \sim (E_{2-} - M_{2-}) \quad ; \quad A_{3/2}(D_{13}) \sim \sqrt{3}(E_{2-} + M_{2-}) .$$

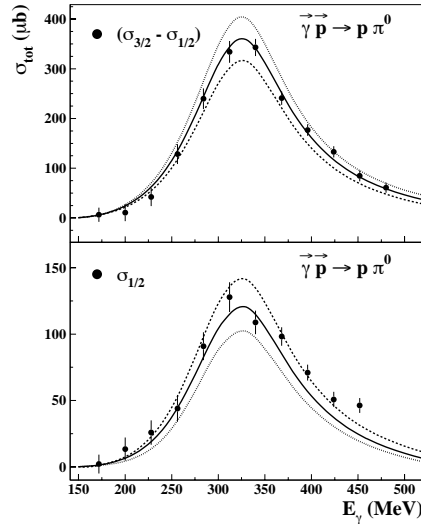


Figure 3. The measured helicity dependent cross sections $\sigma_{31} = (\sigma_{3/2} - \sigma_{1/2})$ (top) and $\sigma_{1/2}$ (bottom) for the $\vec{\gamma}\vec{p} \rightarrow p\pi^0$ reaction are compared to the three different predictions of the HDT model: solid curve: $E2/M1 = -2.5\%$; dashed curve: $E2/M1 = 0$; dotted curve: $E2/M1 = -5.0\%$.

The first double polarized $p\pi^0$ data in the D_{13} region, obtained in the framework of the GDH-experiment, were recently published by our collaboration²⁰. The multipole analysis made with these data produced a significant change in the values of the leading multipoles related to the excitation of this resonance.²⁰

As a further step of this study, the single π^+ was investigated in the second resonance region. Preliminary data on the total unpolarized and polarized cross section are shown in Fig. 4 in comparison with the results of SAID²¹ and MAID²² multipole analyses.

The differences of the two models are much more pronounced in the polarized case. This originates from significant differences in the balance between the non resonant E_{0+} and the resonant E_{2-} multipoles, which enter with opposite signs in the $(\sigma_{3/2} - \sigma_{1/2})$ difference.

4.3. Double pion production

The double pion production channels $p\pi^+\pi^-$, $n\pi^+\pi^0$ and $p\pi^0\pi^0$ were separately analyzed. As an example, the helicity dependent cross sections for the $\gamma p \rightarrow n\pi^+\pi^0$ channel are shown in Fig. 5¹⁷.

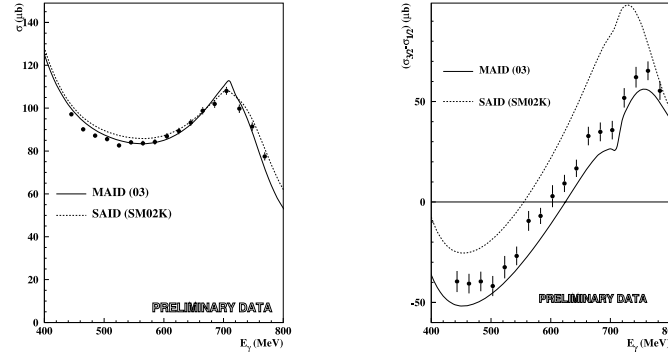


Figure 4. The preliminary unpolarized cross-section (left) and the helicity difference ($\sigma_{3/2} - \sigma_{1/2}$) (right) for the reaction $\gamma p \rightarrow n\pi^+$ are compared with the results of MAID and SAID multipole analyses

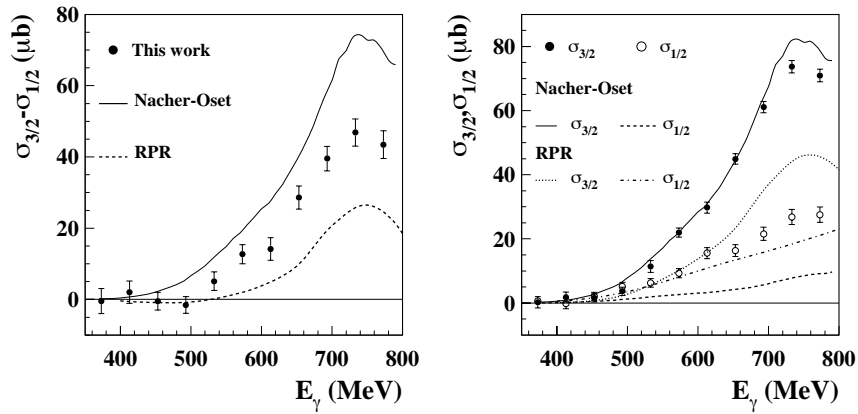


Figure 5. Helicity dependent cross sections for the $\gamma p \rightarrow n\pi^+\pi^0$ reaction. Left: ($\sigma_{3/2} - \sigma_{1/2}$). Right: $\sigma_{3/2}$ and $\sigma_{1/2}$. The different style lines represent the theoretical prediction of the Nacher-Oset²³ and RPR²⁴ models. Data are from¹⁷.

The interesting and previously unexpected feature is the peaking of the cross section at $E_\gamma \sim 700$ MeV or $W \sim 1480$ MeV, definitely below the position of the D_{13} resonance. This is an experimental proof that the two-pion production can not be simply explained by a resonance-driven mechanism (s -channel contribution), but it takes large non-resonant effects such as Born terms and vector meson exchange in the t -channel. It is

also evident that the present models can only describe the data in a semi-quantitative way.

The same is true in the case of the $p\pi^+\pi^-$ reaction. The corresponding data²⁵ are shown in Fig 6 for the separated helicity parts $\sigma_{1/2}$ and $\sigma_{3/2}$. The helicity 3/2 part shows a resonant behavior whereas $\sigma_{1/2}$ is a smoothly rising function of the photon energy. Obviously, this reaction peaks at about 650 MeV, corroborating the statement made above about the complicated nature of the reaction mechanisms.

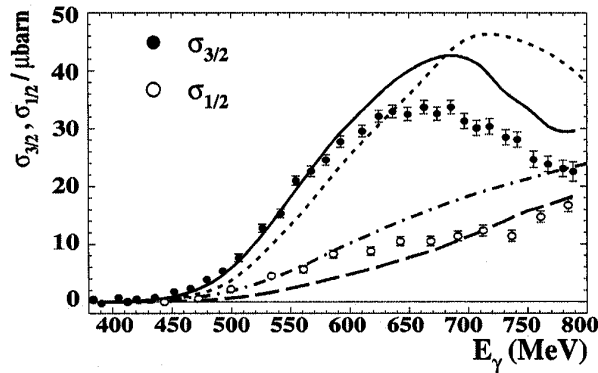


Figure 6. Helicity dependent cross sections for the $\gamma p \rightarrow p\pi^+\pi^-$ reaction. The theoretical predictions are given by the solid and long-dashed lines²³, dashed and dot-dashed lines²⁴.

According to the existing models (see, for instance, Ref. ²³) the large positive $(\sigma_{3/2} - \sigma_{1/2})$ values for the $p\pi^+\pi^-$ channel, are in fact mainly due to an intermediate excitation of a $\Delta\pi$ state, with the D_{13} resonance playing a minor role.

Preliminary data are also available for the $p\pi^0\pi^0$ final state which is of particular interest because of its high sensitivity to the resonance contributions. In this case the intermediate $\Delta\pi$ excitation term is in fact strongly suppressed with respect to the $p\pi^+\pi^-$ and $n\pi^+\pi^0$ reactions and, due to isospin, no intermediate ρ contribution is possible.

There are two models that reproduce equally well the total $p\pi^0\pi^0$ cross section up to about 800 MeV with completely different explanations. The Nacher-Oset model²³ predicts the dominance of the intermediate D_{13} excitation while the Murphy-Laget model²⁶ predicts a dominant excitation of the P_{11} resonance followed by the $P_{11} \rightarrow p\sigma$ and $\sigma \rightarrow \pi^0\pi^0$ decays, where

σ represents a correlated pair of pions in a relative s -wave. A recent paper by Hirata et.al.²⁷ (HKT) has investigated effects of non resonant photo-production concluding that pseudoscalar (PS) πNN coupling is generally found to better reproduce the experimental data than pseudovector (PV) coupling. Our preliminary helicity dependent ($\sigma_{3/2} - \sigma_{1/2}$) cross section data are shown in Fig. 7 and compared to the Nacher-Oset and HKT models. Predictions of the Murphy-Laget model are still not available for this observable.

This last model should however predict a negative behavior for the ($\sigma_{3/2} - \sigma_{1/2}$) difference, while the positive experimental values for this difference imply that a $3/2$ intermediate spin state is dominant.

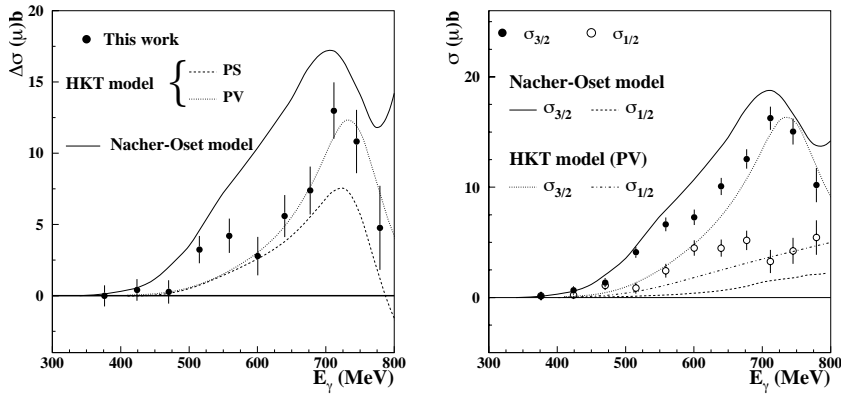


Figure 7. Preliminary helicity dependent cross sections for the reaction $\gamma p \rightarrow \pi^0 \pi^0$. Left: ($\sigma_{3/2} - \sigma_{1/2}$). Right: $\sigma_{3/2}$ and $\sigma_{1/2}$. Data are compared to the predictions of the Oset²³ and HKT (PS or PV coupling)²⁷

According to both Nacher-Oset and HKT models, the D_{13} resonance is largely responsible for the observed dominance of the $\sigma_{3/2}$ cross section, via the process $\gamma N \rightarrow D_{13} \rightarrow \pi \Delta \rightarrow \pi \pi N$. However, as can be seen in Fig. 7, there is also a non-negligible $\sigma_{1/2}$ cross section, which points to significant non-resonant effects and to mechanisms involving the intermediate excitation of additional spin-1/2 resonances, such as P_{11} or $S_{11}(1535)$.

5. Conclusions

For the first time, a large set of high quality double polarization data for the $\gamma N \rightarrow N \pi(\pi)$ channels has been obtained in the first and second resonance

regions in the framework of the GDH experiment.

While the data are in good agreement with the existing theoretical models in the Δ energy region, severe discrepancies were found both on single and double pion photoproduction processes in the $D_{13}(1520)$ resonance region. In the latter case, all theoretical analyses performed up to now were based on unpolarized data, which have a much poorer sensitivity to the lower electromagnetic multipoles than the present data set.

This fact clearly shows the need of precise measurements of the single and double polarization variables for an accurate determination of the properties of all the baryon resonances.

References

1. Review of Particle Physics, S. Eidelman *et al.*, *Phys. Lett. B* **592**, 1 (2004).
2. S. B. Gerasimov, *Sov. J. Nucl. Phys.* **2**, 430 (1966).
3. S.D. Drell, A.C. Hearn, *Phys. Rev. Lett.* **16**, 908 (1966).
4. K. Helbing, these proceedings.
5. O. Jahn, these proceedings.
6. M. MacCormick *et al.*, *Phys. Rev. C* **53**, 41 (1998).
7. J. Ahrens *et al.*, *Eur. Phys. J. A* **21**, (2004), in press.
8. K. Aulenbacher *et al.*, *Nucl. Instrum. Methods A* **391**, 498 (1997).
9. H. Olsen and L.C. Maximon, *Phys. Rev.* **114**, 887 (1959).
10. I. Anthony *et al.*, *Nucl. Instrum. Methods A* **301**, 230 (1991); S. J. Hall *et al.*, *Nucl. Instrum. Methods A* **368**, 698 (1996).
11. C. Bradtke *et al.*, *Nucl. Instrum. Methods A* **436**, 430 (1999).
12. G. Audit *et al.*, *Nucl. Instrum. Methods A* **301**, 473 (1991).
13. S. Altieri *et al.*, *Nucl. Instrum. Methods A* **452**, 185 (2000).
14. M. Sauer *et al.*, *Nucl. Instrum. Methods A* **A378**, 146 (1996).
15. A. Braghieri *et al.*, *Nucl. Instrum. Methods A* **343**, 623 (1994).
16. R. Crawford *et al.*, *Nucl. Phys. A* **603**, 303 (1996).
17. J. Ahrens *et al.*, *Phys. Lett. B* **551**, 49 (2003).
18. J. Ahrens *et al.*, *Phys. Rev. Lett.* **84**, 26 (2000).
19. J. Ahrens *et al.*, *Nucl. Phys. A* **570**, 561 (1998).
20. J. Ahrens *et al.*, *Phys. Rev. Lett.* **88**, 232002 (2002).
21. R.A. Arndt *et al.*, *Phys. Rev. C* **53**, 430 (1996), solution SM02.
22. D. Drechsel *et al.*, *Nucl. Phys. A* **645**, 145 (1999), D. Drechsel *et al.*, *Phys. Rev. D* **63**, 114010 (2001); solution MAID03
23. J.C. Nacher and E. Oset, *Nucl. Phys. A* **697**, 372 (2002); J.C. Nacher *et al.*, *Nucl. Phys. A* **695**, 295 (2001).
24. H. Holvoet, PhD thesis, University of Gent, 2001;
25. M. Lang, PhD. Thesis, University of Mainz, 2004.
26. L. Murphy and J.-M. Laget, report DAPNIA-SPHN-95-42, 1995.
27. M. Hirata, N. Katagiri, T. Takaki, *Phys. Rev. C* **67**, 034601 (2003).